ELONGATIONAL FLOW EFFECT ON THE PERFORMANCE OF BIOMASS POLYMER ALLOYS

RYO SEIRIKI, BIREI TANAKA, TATSUYA TANAKA & MASAHIRO SASADA
Department of Mechanical Engineering and Science, Doshisha University, Japan

ABSTRACT

In the context of environmental conservation, there is an ongoing transition from petroleum-derived plastics to biomass-derived plastics, a shift that encompasses the field of engineering plastics. One example is bio-polycarbonate (Bio-PC). The aim of this study was to enhance the impact strength of PMMA, an acrylic resin that is characterized by brittleness, by alloying it with Bio-PC, a ductile material with excellent impact resistance. In the PMMA/Bio-PC system, which is incompatible and has a two-phase morphology, the dispersion and distribution of the dispersed phase are important for the development of impact resistance properties. In the PMMA/Bio-PC system with different viscosity ratios, the kneading method employing elongational flow has been shown to be effective when composites are produced using a twin-screw extruder. Therefore, a comparison was made between conventional shear kneading and elongational kneading. The results showed that the kneading method using elongational flow was effective in terms of dispersibility, although no significant difference in distributivity was observed. It was found that there is a possibility that further improvement of distributivity in the kneading method using elongational flow can lead to the development of enhanced impact properties.

Keywords: polymer alloy, elongational flow, twin screw extruder, impact strength.

1 INTRODUCTION

A transition from petroleum-derived plastics to biomass-derived plastics is occurring in the context of environmental conservation [1]. This transition encompasses the field of engineering plastics, with notable examples such as the development of Bio-polycarbonate (Bio-PC). Bio-PC is a ductile material with enhanced impact resistance. The alloying of Bio-PC with PMMA, an acrylic resin with inferior impact strength, allows for the creation of a material with complementary properties. The present study aims to enhance the impact strength of PMMA and Bio-PC composites. The incompatibility between PMMA and Bio-PC results in the formation of a Bio-PC phase, which does not dissolve into the PMMA. In the PMMA/Bio-PC system, where a two-phase morphology is observed, the interface between the Bio-PC dispersed particles and the PMMA matrix, a region of concentrated stress when a load is applied, forms a shear zone by shear-yielding of the matrix [2]. This process may absorb the impact of energy, a phenomenon believed to contribute to impact strength [3]. A potential approach to enhance impact strength is to improve dispersibility by refining the dispersed phase [4]. The number of dispersed particles is known to increase with decreasing size of the dispersed phase, and it is expected that this would lead to an increase in shear zones, which would in turn increase the energy absorption rate and improve impact strength.

However, it should be noted that a barrier to impact strength exists, namely cracking between the dispersed particles. It is hypothesized that a critical particle-to-particle distance exists at which cracking occurs between dispersed particles, and that exceeding this distance leads to cracking between particles, thus impeding enhanced impact strength [5], [6]. To prevent fracture due to cracking, uniform distribution of the dispersed particles is necessary [5].

www.witpress.com, ISSN 1743-3509 (on-line)
doi:10.2495/HPSM250021

In polymer composites, the process of melt compounding using a twin-screw extruder is frequently employed. The flow patterns within the twin-screw extruder are characterized by the existence of shear flow and elongational flow, with shear flow exhibiting a dominant presence [7]. The dispersion of PMMA/Bio-PC systems with different viscosities, through the utilization of shearing, has proven to be a challenge [8]. Conversely, it has been observed that elongational flow possesses the capacity to disperse PMMA/Bio-PC systems with different viscosity ratios [8]. The formation of a fine microstructure through elongational flow is expected to stabilize the flow by homogenizing the viscosity and improve the distribution of the dispersed phase. To create an elongational flow field in a twin-screw extruder, a special segment fixed blister disk (XBD) [9] was developed by the authors. After the dispersed phase is dispersed using XBD, the dispersed phase is evenly distributed using a full-flight screw with excellent transport and distribution properties.

In this study, a comparison was conducted between the dispersibility and distributivity of PMMA/Bio-PC systems by elongational kneading using XBD and conventional kneading using kneading disk (KD). Subsequently, to investigate the effect of elongational mixing on the impact strength of the PMMA/Bio-PC system, samples were prepared via elongational mixing and subjected to impact testing.

2 PRELIMINARY KNOWLEDGE

2.1 Comparative experiments between shear kneading and elongational kneading

2.1.1 Theory

Elongational flow is a flow in which a velocity distribution is generated in the flow direction. The dispersion effect of elongational flow in blends of incompatible Newtonian fluids has been demonstrated by Grace [10]. In this experiment, the shear and elongational splitting conditions of a single droplet in a matrix liquid were obtained experimentally, as shown in Fig. 1. The vertical and horizontal axes are the capillary number Ca and the viscosity ratio ρ, respectively, expressed by eqn (1):

$$Ca = {}^{\eta_M \dot{\gamma} \rho}/_{\sigma} \quad , \quad \rho = {}^{\eta_D}/_{\eta_M}. \tag{1}$$

Here, η_M is the matrix viscosity, η_D is the dispersed phase viscosity, $\dot{\gamma}$ is the strain rate and σ is the interfacial tension. Ca is the ratio of the force generated by the matrix flow to the interfacial tension. In other words, it can be recognized as the force that tries to deform the droplet by flow and the force that tries to undo the deformation by the interfacial tension. The solid line in Fig. 1 shows the critical capillary number at which the droplet splits into simple shear flow and simple elongational flow, and the droplet can disperse in the region above the solid line. The results show that the elongational flow is below the critical Ca of the shear flow for all viscosity ratios, which means that the elongational flow can disperse in the region above the solid line. This suggests that elongational flow may be more energetically efficient than shear flow in terms of dispersion. In addition, shear flow cannot split at viscosity ratios above about 5, no matter how much shear action is applied, whereas elongational flow can split over a wide range of viscosity ratios. For this reason, elongational flow has attracted attention in the field of composites. However, shear flow is dominant in melt kneading using a twin-screw extruder, which is often used for composites, and it is necessary to intentionally

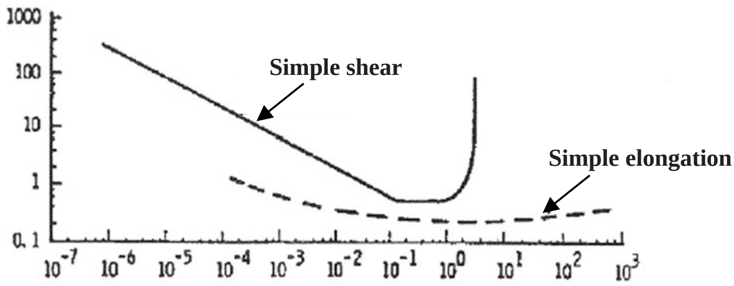

Figure 1: Relation between critical Capillary number and viscosity ratio according to Grace's analysis [10].

generate elongational flow [7]. In previous studies, the rapid expansion and contraction geometry has been used to obtain high elongation rates as a kneading technique using elongational flow [11]. If the polymer flows through a channel with compressive and expansive sections, the flow changes abruptly in the compressive and expansive sections, resulting in a large change in the elongation velocity. As shown in eqn (2) [7], an increase in the elongational strain rate leads to higher elongational stress, which is expected to promote dispersion. In eqn (2), σ_E represents elongational stress, η_E denotes the elongational viscosity, and $\dot{\varepsilon}$ is the elongational strain rate.

$$\sigma_E = \eta_E \dot{\varepsilon}. \tag{2}$$

In this study, the XBD segment (see Fig. 2) was used to generate the predominant elongated flow field within the twin-screw extruder. The XBD has multiple through holes with a diameter of 1.0 mm or less. As shown in Fig. 2, upon insertion of the XBD between the Full Flight Screw, which is a conveying screw, the resin conveyed flows into the multiple through holes. Consequently, the elongation velocity increases with the loss of pressure due to the rapid shrinkage of the flow path, thereby creating a dominant elongational flow field. In this study, twin-screw extrusion experiments were conducted using a screw configuration with an XBD and a conventional KD. These experiments were undertaken to demonstrate the effectiveness of elongational flow. Initially, PMMA/Bio-PC was kneaded using the Full Flight segment screw configuration, which has been shown to have reduced kneading action and superior distribution and conveying capabilities, to prepare materials for comparison.

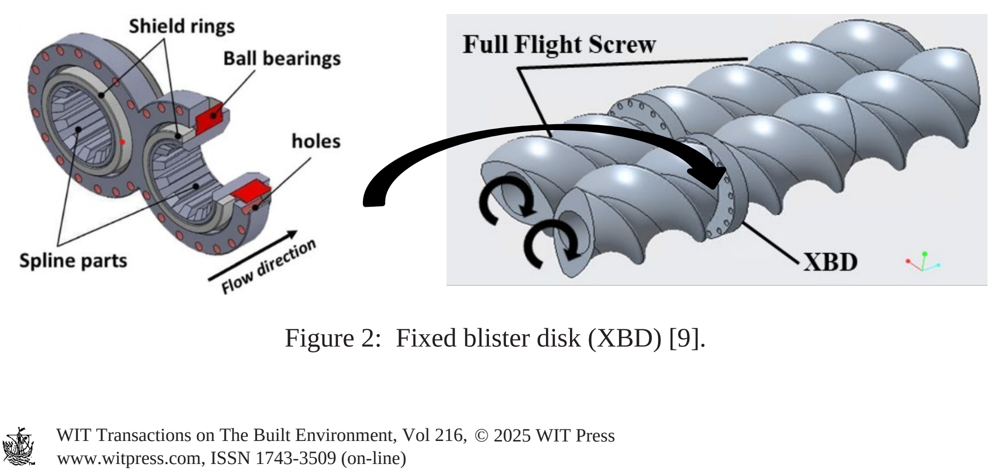

Figure 2: Fixed blister disk (XBD) [9].

Subsequently, the screw configuration was used for elongational kneading with XBD and for shear kneading with KD.

3 MATERIALS AND EXPERIMENTAL PROCEDURES

3.1 Shear kneading and extension kneading

The experimental apparatus comprised a twin-screw extruder (ZSK18, manufactured by Cooperion, Inc.), with a screw diameter of 18 mm, L/D = 40, and a maximum torque of 38 Nm. The operating conditions are detailed in Table 1. The material composition ratio was 50/50 (wt%). Polymethyl methacrylate resin: PMMA (ACRYPET1, Mitsubishi Chemical Corp., VH001) and Bio-polycarbonate: Bio-PC (DURABIO, Mitsubishi Chemical Corp., D7340R) were used as materials. Bio-PC has a density of 1.36 g/cm^3 and an MFR of 2.0 g/10 min (230°C, 3.8 kg). In the experiments, this material was previously kneaded using the full-flight screw configuration shown in Fig. 3(I), which exhibited minimal kneading action. Using the obtained samples, shearing and elongation mixing were carried out. The screw configuration for elongational kneading with XBD is shown in Fig. 3(II), while the screw configuration for shearing kneading with KD is shown in Fig. 3(III). After the extrusion experiments, morphological observations were conducted to compare dispersibility and distribution. The extruded pellets were moulded into a film (100 µm) by a press machine. After moulding, the morphological structure was observed using an X-ray CT (nano3DX, Rigaku Corporation).

Table 1: Operating conditions.

Composition ratio (wt%)		Quantity: Q(kg/h)	Number of rotations: Ns (rpm)	Barrel temperature (°C)
PMMA	Bio-PC			
50	50	2.5	150	220

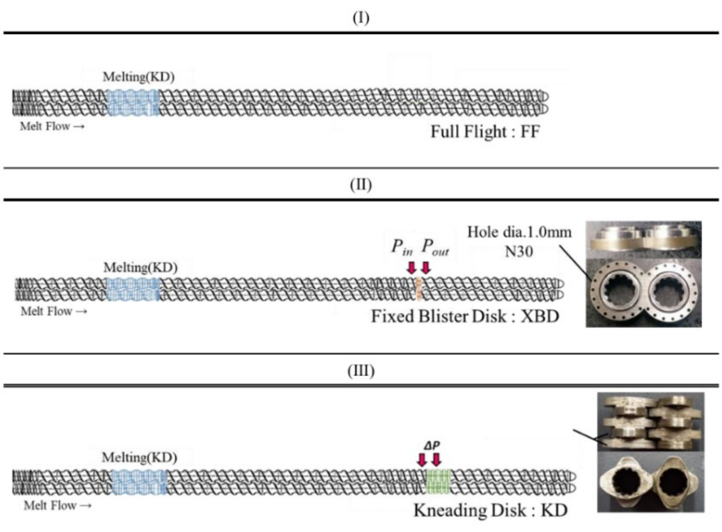

Figure 3: Screw configuration. (I) Distributive extrusion; (II) Elongational extrusion; and (III) Shear extrusion.

3.2 Evaluation of Impact strength

Samples of PMMA/Bio-PC with different composition ratios were prepared by elongational kneading, and dumbbell specimens were moulded using a small injection moulding machine. The specimens were then subjected to Izod testing. A co-axial twin-screw extruder (Thermo Fisher Scientific TSE24 MC Twin-screw Extruder Barrel Dia24, L/D:28) was used for kneading. The screw configuration shown in Fig. 4 was used in the design of the extruder to achieve adequate impact strength. The composition ratio of PMMA/Bio-PC was 90/10 wt%, 80/20 wt%, and 60/40 wt%. The kneading temperature was set at 220°C, the feed rate at 3 kg/h, and the rotation speed at 125 rpm. The pellets obtained from twin-screw extrusion were fed into an injection moulding machine (Thermo Fisher Scientific HAAKE Mini Jet Pro) to produce dumbbell specimens. An Izod impact tester (Impact Tester IT, Toyo Seiki Co., Ltd.) was used for impact resistance tests.

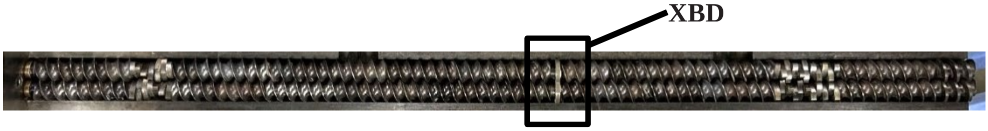

Figure 4: Screw configuration.

4 RESULTS AND DISCUSSION

4.1 Comparison of dispersibility and distributivity between shear kneading and elongational kneading

The morphology of the samples obtained by shear kneading using conventional KD and by elongational kneading using XBD is shown in Fig. 5. Bio-PC with high relative density is white, while PMMA with low density is black. The material produces with Full Flight Screws without kneading does not form a sea-island structure and has a co-continuous structure (Fig. 5(a)), indicating poor dispersion. In contrast, the XBD sample in Fig. 5(b) and the KD sample in Fig. 5(c) form a sea-island structure, indicating that the XBD and KD segments have dispersion performance. Comparing the XBD and KD samples, the XBD sample tends to have a finer dispersed phase size than the KD sample. Fig. 6 shows the average dispersed phase size and frequency distribution of the XBD and KD samples. The average dispersive phase size of the XBD sample was 5.35 μm^2, and that of the KD sample was 39.9 μm^2. Fig. 6(a) shows that the dispersed phase of XBD is approximately 86% smaller than the KD sample. Furthermore, Fig. 6(b) and (c) show that the slope of the cumulative frequency distribution of the XBD sample is greater than that of the KD sample, indicating that the uniformity of the dispersed phase size is superior. These results indicate that elongational kneading using XBD is superior to shear kneading using KD in terms of making the size of the dispersed phase finer and more uniform. Moreover, the results suggest that elongational kneading using XBD is effective for the dispersibility of PMMA/Bio-PC composites.

A box-counting method using ImageJ software was used to obtain the fractal dimension and estimate distributivity. The observed image is equally divided into squares of side r, and a set of boxes is generated. If $N(r)$ is the number of boxes containing even a small amount of dispersive phase, it is known that the relation in eqn (3) holds [12]:

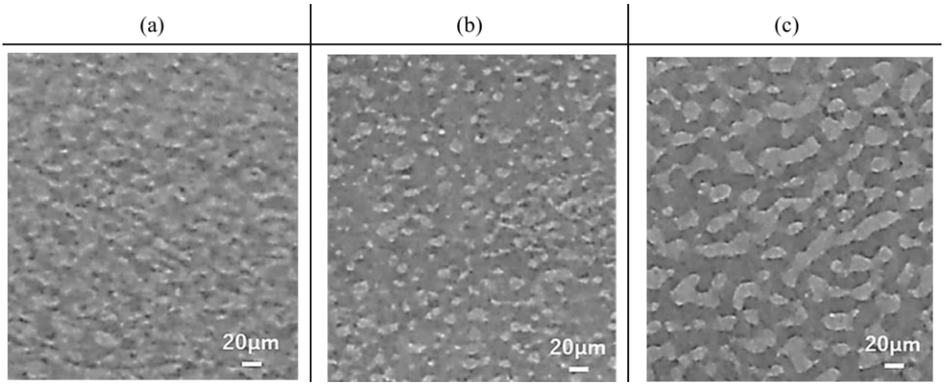

Figure 5: Morphology of materials from each extrusion method. (a) Distributive extrusion; (b) Elongational extrusion; and (c) Shear extrusion.

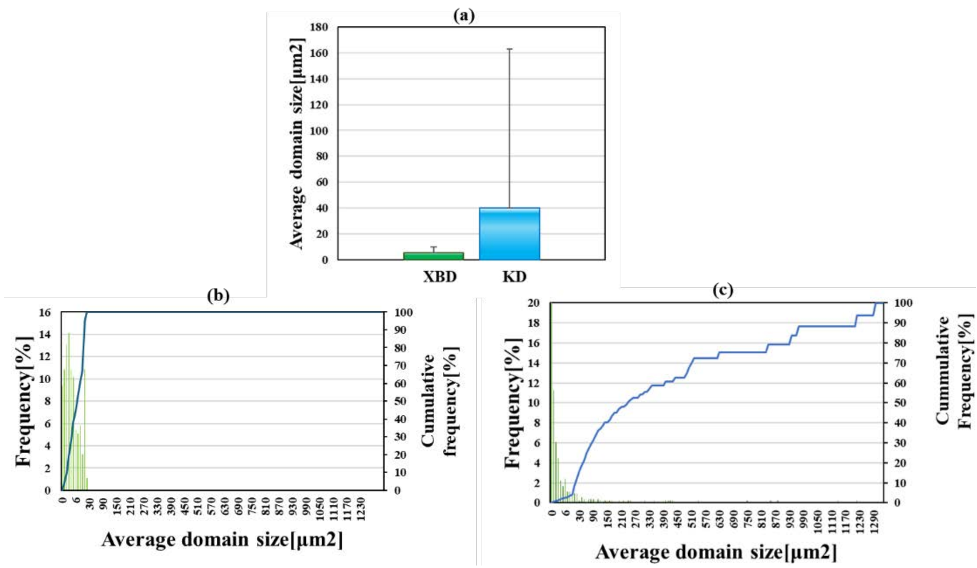

Figure 6: Differences in dispersed phase due to different extrusion methods. (a) Average domain size (average and standard deviation of measurements); (b) XBD; and (c) KD frequency distribution and cumulative frequency distribution.

$$N(r) = k \cdot r^{-D}. \tag{3}$$

In eqn (3), D is the fractal dimension and k is a constant. The box-counting method is a method of measuring $N(r)$ for each r by changing the value of r, plotting the relationship between $r$and $N(r)$ on a log–log graph, and obtaining D from its slope [12]. The observed image was 390 × 425 pixels, and the box was analysed by setting r to 4, 8, 16, 32, and 64. As a result, D of the KD sample was 1.698, and that of the XBD sample was 1.622, showing no significant difference in distributivity.

4.2 Impact strength

4.2.1 Comparison of impact strength

The impact strength results obtained from the Izod impact test are shown in Fig. 7. These results indicate that no significant improvement in impact strength was observed for any composition ratio. The impact strength mechanism of the PMMA/Bio-PC system is thought to involve the formation of shear bands when stress is applied [2]. Specifically, stress is concentrated at the interfaces of the dispersed particle, causing shear yielding of the matrix resin, resulting in the formation of shear bands that absorb impact energy, thereby enhancing impact strength [3]. Therefore, finer dispersion of the dispersed phase increases the number of dispersed particles, leading to a higher occurrence of shear bands, which improves energy absorption and ultimately enhances impact strength. When a load is applied to a PMMA/Bio-PC alloy, a stress concentration occurs at the tip of the plastic deformation region of the matrix surrounding the dispersed particles. When this stress concentration exceeds the crazing stress σ_c of the matrix resin, crazing form between the particles. As the load increases, these crazes grow into cracks, eventually leading to abrupt failure and acting as a barrier to increased impact strength. There is a critical interparticle distance d_l between dispersed particles at which cracking occurs, and cracking occurs between particles when the distance between dispersed particles exceeds this distance. d_l is shown in eqn (4) [5]:

$$d_l = 2R\exp\left\{\frac{\frac{\sigma_c}{\tau_0}-1}{2}\right\}. \quad (4)$$

In eqn (4), d_l is the critical interparticle distance, R is the average particle radius, σ_c is the crazing stress of the resin, and τ_0 is the shear yield stress of the resin. To prevent crack initiation, it is necessary to keep all interparticle distances below d_l through uniform distribution of the dispersed phase. In the next subsection, a uniform distribution model is developed, and morphological observations are made to study the distribution and dispersion aspects.

4.2.2 Uniform distribution model

A uniform distribution model was created for each composition, and the model’s interparticle distance was compared with the critical interparticle distance. As shown in Fig. 8, the uniform

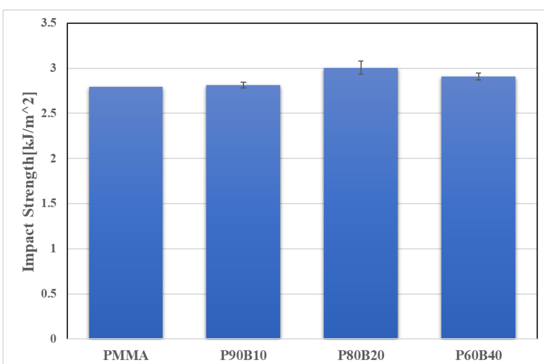

Figure 7: Impact strength for PMMA/Bio-PC weight composition ratio.

distribution model considers the case where a cubic lattice with a side d containing a particle at the center is laid out in a green cube with a side of 10 μm. In this case, the distance between the centers of the particles can be expressed by d. When the weight ratio of PMMA/Bio-PC is 90/10 wt%, the volume ratio is 91.1%/8.9%, so the volume V_B of Bio-PC in the cube V $=1000\mu m^3$ is:

$$V_B = 1000 \times 0.089 = 89\ [\mu m^3]. \tag{5}$$

If the radius of the dispersed particles is R, the volume V_P per dispersed particle can be expressed as follows:

$$V_P = \frac{4\pi R^3}{3}\,[\mu m^3]. \tag{6}$$

The number of dispersed particles that can exist in the cube can be expressed as eqn (7), considering eqns (5) and (6):

$$\frac{V_B}{V_P} = 89 \times \frac{3}{4\pi R^3} = \frac{267}{4\pi R^3}. \tag{7}$$

In the case of uniform distribution, the volume V_N of the cubic lattice that a single dispersed particle enters is:

$$V_N = V \times \frac{V_P}{V_B} = V \times \frac{4\pi R^3}{267} = \frac{4000}{267}\pi R^3 [\mu m^3]. \tag{8}$$

Since the length of a side of the cubic lattice containing a dispersed particle can be considered to be equal to the distance between the dispersed particles, the distance d_{P1} between dispersed particles can be obtained from eqn (8) as follows:

$$d_{P1} = \sqrt[3]{V_N} = \sqrt[3]{\frac{4000}{267}\pi}\ \ R \fallingdotseq 3.61R. \tag{9}$$

Considering PMMA/Bio-PC weight composition ratio of 80/20 wt% and 60/40 wt%, $d_{P2} = 2.85R$ and $d_{P3} = 2.25R$, respectively.

Substituting the craze generation stress $\sigma_c = 68$MPa and the shear yield stress $\tau_0 = 39MPa$ [5] for the matrix resin into eqn (4), the critical interparticle distance d_l can be expressed as:

$$d_l = 2.90R. \tag{10}$$

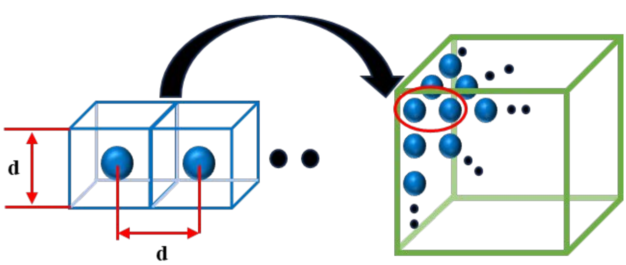

Figure 8: Uniform distribution model.

The results show that $d_{P1} > d_l$ for PMMA/Bio-PC = 90 wt%/10 wt%. Therefore, even with uniform distribution, the interparticle distance is always greater than the critical interparticle distance, and cracks are expected to occur and impact strength cannot be improved. On the other hand, when PMMA/Bio-PC = 80/20 wt% or 60/40 wt%, $d_P < d_l$, the interparticle distance is less than the critical interparticle distance when uniformly distributed. This result suggests that an increase in impact strength can be expected at a Bio-PC content of approximately 20 wt% or more. However, the impact strength was not improved at either 80/20 wt% or 60/40 wt%. This result is discussed by focusing on the phase dispersion and distribution from actual morphology.

4.2.3 Evaluation of phase dispersion and distribution by morphological observation

Observations of the dispersed phase were made using a field emission scanning electron microscope (JEOL Ltd. FE-SEM, JSM7001FD). The observation results shown in Fig. 9 indicate that all materials have a sea-island structure. However, the size of the dispersed phase in the PMMA/Bio-PC = 60/40 wt% case is not uniform, indicating that the dispersibility is poor. To visualize the dispersibility, the dispersed particle size and the number of dispersed particles were examined by analysis using ImageJ software. A graph of the number of dispersed particles is shown on Fig. 10. Fig. 10(a) shows the number of dispersed particles, and Fig. 10(b) shows a frequency graph of the dispersed particle diameter. The maximum number of dispersed particles was 1207 for PMMA/Bio-PC = 80/20 wt%, and the minimum was 139 for PMMA/Bio-PC = 60/40 wt%. From the frequency graph of the particle size distribution, it can be seen that the 80/20 wt% sample has the highest number of particles with a diameter of 0.50 μm or less, and that the variation in particle size distribution is also the smallest for the 80/20 wt% sample. It can be seen that the 60/40 wt% sample has the lowest number of particles with a diameter of 0.50 μm or less, and that the variation is the largest. These results indicate with an 80/20 wt%, the particle size can be reduced while controlling the variation in particle size, and the dispersion is good. On the other hand, with a 60/40 wt%, it is believed that it is difficult to reduce the dispersion phase and increase the number of particles. Furthermore, from the observation images, it can be seen that the large aggregates do not have a circular shape, but an irregular shape. From these results, it can be concluded that the dispersion is poor. This is thought to be due to the high content of Bio-PC. When the Bio-PC content is 40 wt%, even when an elongation kneading process is used, it is thought that dispersion is difficult, although it has on an island-in-the-sea structure. This suggests that a high content of Bio-PC may not be suitable for improving the impact resistance properties.

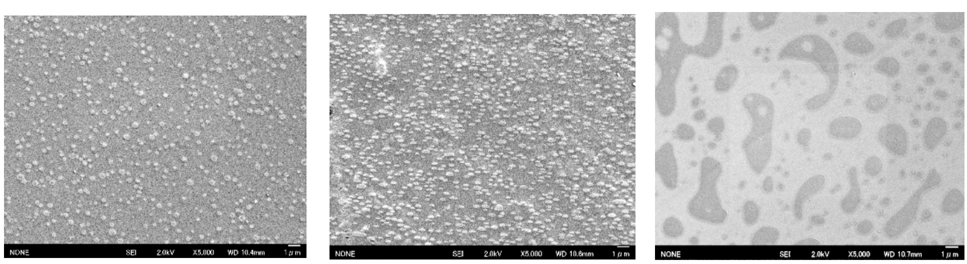

(a) (b) (c)

Figure 9: Morphological observation images for each composition ratio. (a) PMMA/Bio-PC = 90/10 wt%; (b) 80/20 wt%; and (c) 60/40 wt%.

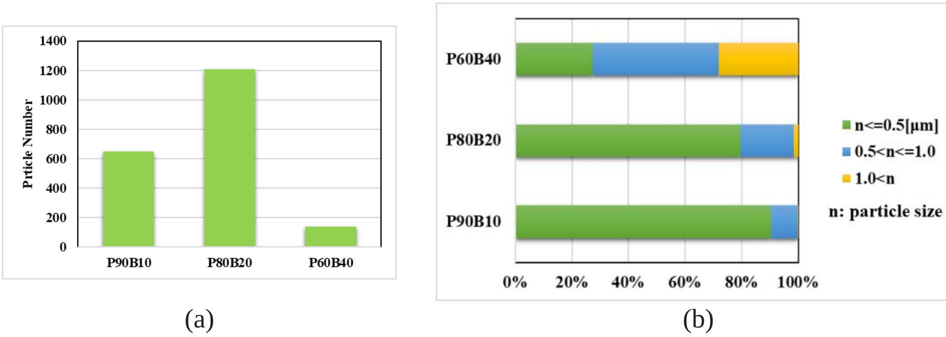

Figure 10: (a) Number of dispersed particles for each composition ratio; and (b) Particle size distribution for each composition ratio.

The distance between particles was measured for PMMA/Bio-PC 80/20 wt% and 60/40 wt%. It was assumed that the distance between particles was the distance between the centres of gravity. This was obtained by analysing the SEM images in Fig. 9 and estimating the centre of gravity coordinates using ImageJ software. For the 80/20, the average particle diameter was extracted, and for the 60/40, because there was a lot of variation, the particle closest to the most frequent value was selected, and then three particles close to the target particle were selected and the distance was measured, after which the average of the three was taken.

The distance between the dispersed particles and the critical particle distance was then compared. Substitution of 0.221 μm, which is the average dispersion phase radius for 80/20 wt%, into eqn (4) yielded a critical particle distance of 0.640 μm. Similarly, for 60/40 wt%, the critical particle distance was determined to be 1.04 μm. The relationship between the measured particle distance and the critical particle distance is illustrated in Fig. 11. The bar graph contains the critical particle distance and symbols for the measured particle distance. The results show that for the 80/20 wt% mixture, approximately 60% of the measured particle distances exceeded the critical particle distance. From these results, it is

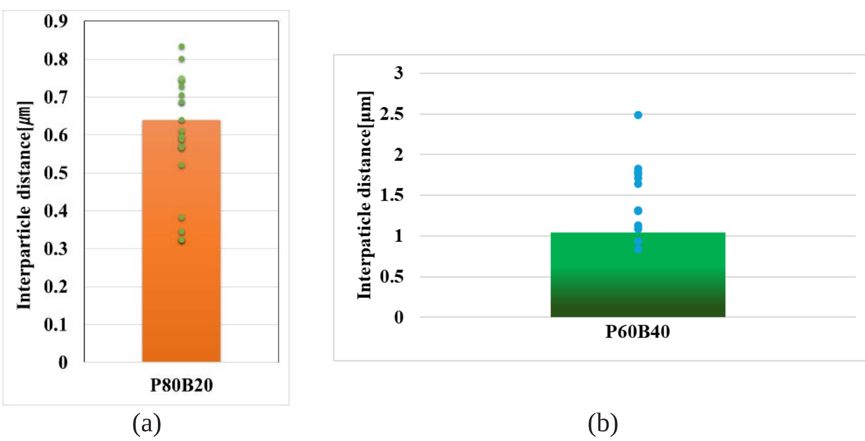

Figure 11: Relationship between critical interparticle distance and measured interparticle distance for PMMA/Bio-PC. (a) 80/20 wt%; and (b) 60/40 wt%.

thought that the occurrence of cracks due to poor distribution when impact is applied inhibits the development of impact resistance. In the 60/40 mixture, approximately 83% of the particles exceed the critical particle-to-particle distance. These results suggest that increasing the content of Bio-PC to 40 wt% or more will worsen dispersion and distribution, making it difficult to impart impact resistance. Based on the above, it is thought that the optimal content for designing impact resistance in PMMA/Bio-PC composite materials using elongational flow is between 20 wt% and 40 wt%. However, this study has shown that distribution is still poor.

Based on the results of this study, it is necessary to look for optimal conditions that also improve the distribution to achieve higher impact strength. One factor that the effects distribution properties is the residence time in the twin-screw extruder [13]. By changing the operating conditions of the twin-screw extruder, it is possible to control the residence time of the molten resin. While it is believed that it is possible to improve the distribution by these operations, it is believed that it is necessary to consider the effect of changes in operating conditions on the elongation effect. Changes in flow near the XBD may affect the elongation effect and change the distribution. Although it is difficult to visualize the flow condition near the XBD, there is a correlation between the elongation stress and the pressure loss before and after the XBD, and it is supposed that it is possible to understand the elongation effect by obtaining the pressure from the experiment. The elongation stress and pressure loss can be related by the following formula [14]:

$$\sigma_E = {}^3\!/_8\,(n+1)\Delta P \quad 3-2-3-1, \tag{11}$$

where σ_E is the average elongation stress, n is the non-Newtonian index, and ΔP is the pressure loss. From this equation, it is possible to indirectly evaluate the effect of changes in operating conditions on the elongation effect by measuring the pressure. In the future, it will be necessary to establish the optimal values for the elongation effect and residence time required for dispersion and distribution to enhance the impact strength, with the amount of Bio-PC added between 20 wt% and 40 wt%.

5 CONCLUSION

In this study, the effect of elongation on PMMA/Bio-PC composites was investigated, with a comparison being made between the dispersibility and distributivity of composites produced by conventional shear mixing using KD and elongation mixing using XBD. In the case of elongation mixing using XBD, there was no significant difference in distributivity was observed when compared to shear mixing, however the refinement of the dispersed phase in terms of dispersibility was confirmed. Subsequently, the effect of the composition ratio of PMMA/Bio-PC on impact strength was measured, using XBD-based elongation mixing. The study revealed that there was no enhancement in impact strength across all composition ratios. However, although the need to improve the dispersibility remains, it was estimated that the optimal content range of Bio-PC for designing PMMA/Bio-PC composite materials with improved impact resistance through elongation flow is between 20 wt% and 40 wt%.One factor affecting the phase distribution is the residence time in the twin-screw extruder. By changing the operating conditions of the twin-screw extruder, it is possible to control the residence time of the molten resin. Whilst it is believed that improvements can be made to the distribution through these operations, it must be considered the effect of changes in operating conditions on the elongation effect. In future research, it will be necessary to establish the optimal values for the elongation effect and residence time required for dispersion and distribution to enhance the impact strength.

ACKNOWLEDGEMENTS

I would like to express my gratitude to Professor Tanaka and Professor Sasada for providing me with various opportunities and valuable advice throughout this research. I would also like to extend my appreciation to Ms Birei Tanaka and Ms Yuki Masaki for their invaluable cooperation as collaborative researchers.

REFERENCES

[1] Yoshida, M., Development and prospects of bioplastics. *Japan Society of Material Cycles and Waste Management (JSMCWM)*, **30**(2), pp. 123–130, 2019.
[2] Narisawa, I., Ishikawa, Y., Ishikawa, T. & Ogawa, H., Fracture and crazing of polymers under plane strain. *Polymer Journal*, **36**(8), pp. 543–556, 1979.
[3] Narisawa, I. & Kuriyama, T., Impact and fatigue properties of polymer blends. *Journal of the Society of Rubber Industry, Japan*, **68**(12), pp. 875–882, 1995.
[4] Hayashi, T., Watanabe, T., Tanaka, H. & Toshio, N., Morphology and mechanical properties of three-component immiscible polymer alloys. *Polymer Journal*, **49**(4), pp. 373–382, 1992.
[5] Ishikawa, Y., Morphology design for impact strength improvement. *Polymer Journal*, **40**(10), pp. 680–683, 1991.
[6] Hisamatsu, T., Nakamo, A., Ishikawa, Y. & Iwakura, K., Analysis of stress concentration relaxation mechanisms in polymer alloys by plastic mechanics. *Seikei-Kakou (Journal of the Japan Society of Polymer Processing)*, **11**(3), pp. 187–193, 1989.
[7] Tanaka, T. & Matsumoto, K., Kneading and dispersion technology of nanocomposites and polymer blends utilizing extensional flow in twin-screw extruders. *Advanced Functions of Plastics and Multiphase Flow*, **38**(2), pp. 114–121, 2024.
[8] Kajiwara, T., Theory and computer simulation of melt mixing for polymeric materials. *Proceedings of the 60th National Congress of Theoretical and Applied Mechanics*, 2011.
[9] Matsumoto, K. & Tanaka, T., A modified blister mixing element for generating extensional flow in a twin-screw extruder: Process characterization and dispersion state of carbon nanotubes in cyclo-olefin polymer. *Polymer Engineering and Science*, **62**(4), pp. 1223–1238, 2022.
[10] Grace, H.P., Dispersion phenomena in high viscosity immiscible fluid systems and application of static mixers as dispersion devices in such systems. *Chem. Eng. Commun.*, **14**(3–6), pp. 225–277, 1981.
[11] Tokihisa, M., Yakemoto, K., Sakai, T., Utracki, L.A., Sepehr, M., Li, J. & Simard, Y., Extensional flow mixer for polymer nanocomposites. *Polym. Eng. Sci.*, **46**, pp. 1040–1050, 2015.
[12] Fujimoto, K., Yamamoto, T. & Shioya, T., Evaluation of fracta1 dimensions of fracture surfaces using box-counting method. *Mechanical Engineering Congress*, **6**, pp. 66–67, 2006.
[13] Hirofumi, T., Mikata, Y., Matsuda, S. & Atsushi, M., Dispersion of carbon-nanotubes in a polymer matrix by a twin-Screw extruder. *Journal of the Society of Plastic Engineering Japan*, **14**(2), pp. 126–131, 2002.
[14] Matsumoto, K., Study on dispersive mixing for nanocomposite materials with co-rotating twin-screw extruder. PhD Dissertation, Doshisha University, 2017.